Pyrolysis of Large Mallee Wood Particles: Temperature Gradients within a Pyrolysing Particle and Effects of Moisture Content

MD Mahmudul Hasan, Xun Hu, Richard Gunawan and Chun-Zhu Li *

Fuels and Energy Technology Institute, Curtin University of Technology, GPO BOX U1987, Perth, WA 6845, Australia

*Corresponding author:

Email address: chun-zhu.li@curtin.edu.au

Phone: +61 8 9266 1131

Fax: +61 8 9266 1138

September 2016

Abstract

Temperature profiles inside a large pyrolysing particle were studied and are reported in this paper. Mallee trunks of similar diameter from the same tree were used to prepare cylindrical samples with 40 mm length. A fluidised-bed reactor was used to pyrolyse the large particle. The temperature profiles inside the particle were recorded during pyrolysis to allow the calculation of corresponding heating rate profiles inside the particle. The effects of moisture were studied by pyrolysing some particles with 15 to 20% moisture content. The temperature profiles obtained from the pyrolysis of dry and wet samples have been compared to identify the possible effects of moisture on the temperature profiles. A possible change in the thermal conductivity of the wood was identified around 100°C, which caused a peak in the heating rate profile. Some possible exothermic peaks were observed at around 325°C and 425°C. A peak in the heating rate profile at around 200°C in the case of the pyrolysis of wet particles was believed to be related to the changed 3-D macromolecular structure of the biomass in the presence of moisture. Some yields of tar and char along with other analytical results were presented to support our observations on the temperature profiles.

Keywords: Pyrolysis; Large particles; Mallee wood; Temperature profile; Heating rate; Moisture.

1. Introduction

Pyrolysis of biomass has been studied extensively during the last several decades with a special focus on fast pyrolysis [1 – 5]. While fast pyrolysis achieves fast heating rates of biomass particles to give high bio-oil yields, biomass feedstock must be pulverised into very fine powders to reduce intra-particle heat and mass transfer resistances. The energy intensive and thus costly pulverisation, as part of feedstock preparation, frequently becomes a significant hurdle for the commercialisation of fast pyrolysis technologies. It has now become clear that the pyrolysis of relatively large particles at relatively low temperatures may be an attractive alternative for the utilisation of non-food lignocellulosic biomass resources.

Overcoming the heat and mass transfer resistance within a pyrolysing biomass particle is the key to develop an efficient pyrolysis technology for the utilisation of biomass resources with large particle sizes. Some studies on the pyrolysis of large biomass particles have been reported in the literature [6 – 10], including significant efforts to measure the temperature profiles (gradients) inside a pyrolysing biomass particle. These careful measurements have revealed the presence of both endothermic and exothermic processes taking place in a pyrolysing biomass particle. While the endothermic nature of pyrolysis is commonly accepted due to the needs to break various bonds during pyrolysis, the exact causes of exothermicity are not clear. Park et al. [11] and Bennadji et al. [12] have attributed the observed exothermicity in the temperature profile to the decomposition of solid intermediates before the formation of stable char product. Alternative explanations have also been proposed; examples include peak lignin decomposition [8, 10, 13] after 400°C, secondary tar cracking [14] and release of sensible heat from biomass at the centre of a pyrolysing particle [15]. A

recent study done by Di Blasi et al. [16] investigated the pyrolysis of a cylindrical packed bed of beech wood pellets and observed exothermic, endothermic and exothermic events in the centre of the bed. The exact causes of exothermic reactions remain a debate in the literature.

It should be pointed out that the identification of endothermic or exothermic reactions in the literature has often ignored the physical processes that could also cause apparent exothermic/endothermic events, as will be demonstrated in this study.

Due to the significant temperature gradients within a large pyrolysing biomass particle, from the low temperature in its centre to the high temperature at its outer surface, the products from the pyrolysis of the biomass in the centre will have to undergo secondary reactions as they travel through a porous layer of nascent char and experience increasing temperature. These intra-particle secondary reactions will alter the product distribution [1]. The presence of moisture in the biomass, requiring substantial amounts of energy to evaporate, would necessarily change the temperature gradients/profiles in the particle and in turn change the product distribution. Little information exists in the literature about the effects of moisture content on the temperature profiles in a pyrolysing biomass particle and on the final product distribution.

The objective of this paper is to investigate the temperature profiles in a pyrolysing large biomass particle in the low temperature ranges of 300 to 400^{o}C. The use of temperature derivatives with respect to time, i.e. heating rates, across a pyrolysing particle gives clear information for the identification of endothermic and exothermic events in the particle. Particular efforts have been made to examine the pyrolysis behaviour of wet biomass particles, in comparison with that of dry particles. The pyrolysis products were quantified and characterised with a number of analytical techniques. The results provide new insights into the endothermic and exothermic events in a pyrolysing particle and the effects of moisture

content on temperature gradients and product distribution.

2. Experimental

2.1. Biomass samples

The feedstock for this experiment was the Western Australian mallee eucalyptus *loxophleba* (subspecies *lissophloia*). After removing the bark from the branch, it was cut into 40 mm long pieces that produced cylindrical wood samples with different diameters (exact diameters are given in the figure captions). These samples were then stored into a freezer to avoid microbial degradation. The typical key properties of the wood sample include: 42.4 wt% cellulose, 23.8 wt% hemicellulose, 24.7 wt% lignin with balance amounts of extractives [17]. The typical elemental composition of the feedstock (daf basis) is as follows: 48.4 wt% C; 6.3 wt% H; 0.1 wt% N and 45.2 wt% O (balance) [2].

The wood samples were dried in an oven at 105°C for 24 hours before the pyrolysis experiment. The dried samples were then taken out from the oven just before the experiment. Two samples with similar diameter were used for each experiment, one for pyrolysis and the other for moisture content measurement. While one sample was drilled to put thermocouples inside, the other one was kept aside to make sure both of them experienced the same atmospheric environment. Drilling the sample and inserting thermocouples were done within a short period of time. Both samples were then kept in a closed vessel until the experiment to prevent further moisture adsorption from the

environment. When the reactor temperature was ready, the sample with thermocouples inserted was fed into the reactor. The other sample was weighed at that point and dried later to measure the moisture content.

Experiments were also carried out using wet samples. It was found that the original wood samples contained about 15 to 20% moisture before they were stored in the freezer. Therefore, samples for the experiments with wet mallee wood particles were directly taken out from the freezer just few hours before the experiment. They were kept in a closed bottle in the ambient environment to bring the temperature of the sample back to ambient temperature. The same procedures as outlined above for the pyrolysis of dry samples were followed for the pyrolysis of the wet samples. The possible effects of adsorbed oxygen (during storage) on the heating rate profiles would be negligible because the adsorbed oxygen would have been removed during the initial heating up, long before the particle reached the pyrolysis temperature.

2.2. Experimental setup

A specially designed quartz fluidised-bed reactor was used to pyrolyse single large mallee wood particles. The use of a fluidised-bed reactor ensured relatively stable isothermal temperature environment surrounding the pyrolysing biomass particle. A schematic diagram of the experimental setup is shown in Figure 1. The diameter of the fluidised-bed section was 50 mm with a length of 150 mm. The minimum fluidisation velocity of the setup was 0.02 m/s at normal temperature. The reactor was heated with an electric furnace. Argon was used as the fluidising gas, which was introduced from the bottom of the reactor at a flow rate of 2.5 litre/min. 200 g silica sand with 250 – 350 µm particle sizes was used as the bed material. Un-

fluidised sand bed height was 73 mm, which was enough to cover the whole mallee particle.

The top opening of the reactor was closed using a high temperature silicon cork. Thermocouples (described in the following section) were inserted through the cork. Due to the elastic properties of the silicon, good sealing was achieved even after the thermocouples were inserted through the cork. The mixture of pyrolysis volatiles, non-condensable gases and inert fluidising gas had to go through a condensation train where a mixture of chloroform and methanol was used to trap the volatiles [18]. The first condenser was immersed in ice and the following two were cooled with dry ice to make sure that most of the (heavy) volatiles are trapped.

After the readings from all thermocouples have passed their final peaks and reached relatively stable values, the reactor was then taken out from the furnace and left outside to cool down naturally. During cooling, the flow of argon gas was continued to maintain inert atmosphere inside the reactor to avoid any combustion of char.

2.3. Temperature measurement

Type-K (chromel-alumel) thermocouples were used to measure the temperature in sand bed and in the biomass sample. Two sets of thermocouples inserted through two different corks were used during one experiment (Figure 2). A band of three thermocouples passing through a cork (Figure 2B) was placed into the sand bed at different depths to monitor the heating up of the bed. When the temperature of the sand bed at every depth became ~~very close and~~ steady, the thermocouple bundle including the cork was quickly replaced with another set of thermocouples (Figure 2A) connected to the mallee wood sample. Usually four thermocouples were inserted into a wood cylinder sample at different radial positions but to

the same depth. As the thermocouples were inserted at different radial locations and were tightly fitted into the drilled holes, they were able to hold the sample in position in the fluidising sand bed. At least one thermocouple was placed outside the sample to monitor the temperature profile of the surrounding sand bed during pyrolysis. As the diameter of the thermocouples was only 1.0 mm, the effects of thermal inertia and conductivity would be negligible on the measurements. The thermocouples were connected with a digital multi-channel data logger that could record the data at a maximum sampling rate of five times per second.

2.4. Selection of pyrolysis temperature

A temperature range of 300 to 400°C was selected for the current study with two reasons. Firstly, this is the range of temperatures relevant to the production of bio-oil and biochar. Secondly, this range of temperatures could ensure the authenticity of the data collected on the temperature profile within a pyrolysing particle. To study the temperature profile in a wood sample at a certain location requires fixing the thermocouple with the pyrolysing biomass or char. It is important to make sure that the thermocouple stays in contact with the pyrolysing biomass/char at all times to be able to get reliable data. Many past pyrolysis studies with large particles [6 – 10] have used high temperatures or high heat intensity. It was found in our laboratory during the initial trials that the pyrolysing char would fragment at >400°C. The fragmentation would expose most of the thermocouples to the fluidising sand bed. Therefore, the measured temperature did not always represent the real particle temperature. Char samples produced from our low temperature pyrolysis experiments were found in whole pieces and all the thermocouples were found inside the char.

2.5. Yield determinations

As the volatiles (mainly bio-oil or tar) were trapped using a solution of chloroform and methanol, the determination of tar yield required the evaporation of solvents [18]. Some small amount of tar solution was taken into an aluminium pan and placed in an oven at 35°C for 4 hours in flowing nitrogen. This condition experimentally defined the "tar yield" in this study, which did not include the very volatile light organics. This procedure was repeated three times and an average value was considered. The concentration of tar in the solution and the total amount of tar solution were then used to calculate the tar yield based on the dry weight of the biomass sample.

Char was found as a whole piece after every experiment, which was taken out of the sand bed. The thermocouples were carefully removed from the char. Any sand caught in the cracks of the char was also removed before weighing the char. The char yield was calculated based on the dry weight of the biomass sample.

2.6. Tar analysis

Tar was analysed by gas chromatography – mass spectrometry (GC-MS) and UV-fluorescence spectroscopy. An Agilent GC-MS (6890 series GC with a 5973 MS detector) equipped with a capillary column (HP-INNOWax) was used to analyse the tar solution. The original tar solution was used to prepare 5-6% (accurately known) concentration solution in acetone for injection into the GC-MS. The method used to analyse the samples is described elsewhere [19, 20]. Standard solutions were injected to confirm peak identification and to get the calibration curves for quantification purposes.

A Perkin-Elmer LS50B luminescence spectrometer was also used to analyse the tar sample. A 4-ppm tar sample solution was prepared by diluting the tar solution with the UV grade methanol. A constant energy difference of -2800 cm^{-1} with a scan speed of 200 nm/min was used to record the fluorescence synchronous spectra. The excitation and emission slit widths were both set at 2.5 nm. Each reported spectrum represents the average of four scans.

3. Results and Discussion

3.1. An overview of temperature profiles

Figures 3 to 5 show some typical temperature profiles within the pyrolysing wood cylinders. Readings from five thermocouples are normally presented: four thermocouples in the biomass particle positioned at ~12.5 (i.e. the central line of the cylinder), 9, 6 and 3 mm from the outer surface and one thermocouple placed outside (2-3 mm away from the surface) of the wood cylinder (i.e. at the interface of biomass and the sand bed). As soon as the biomass was immersed into the fluidised-sand bed, the reading from the thermocouple at the outer surface of the wood would increase rapidly. However, before the reading had reached the sand temperature, it started to drop, signalling the commencement of rapid heat transfer from the sand bed to the particle. This heat transfer in turn made the temperature at the biomass-sand bed interface to drop. As the biomass was heated up and the heat flow from the sand to biomass decreased due to the reduced temperature difference, the reading from this thermocouple then gradually increased until it reached a value close to the sand bed

215 temperature.

The reading from the four thermocouples positioned at different radial positions in the wood cylinder showed non-linear heating rates at each location. Furthermore, the time-temperature histories also varied greatly from one radial location to another. While the biomass close to the outer surface has reached very high temperature (e.g. close to 200°C in
220 Figure 5A) and started pyrolysis, the biomass at the centre was still at room temperature. These data clearly indicated that the biomass at the outer surface would have experienced entirely different heating rates and somewhat different reaction pathways from the biomass at the centre of the particle. The details will be discussed below.

The immediate striking feature in these temperature profiles in Figures 3 to 5 was the
225 peak temperature reached at each temperature. For example, at the sand temperature of 300°C (Figure 3), while the temperature 3 mm away from the outer surface finally reached the sand temperature, the temperature at the centre went up to 330°C, well above the sand temperature of 300°C. These observations clearly confirm the previous report [16] about the presence of exothermic reactions during pyrolysis even at temperatures as low as 300°C. In
230 each case, the difference between the observed peak temperature and the sand temperature increased with increasing distance from the outer surface.

Figure 6 shows that the difference between the peak temperature at the centre and the sand temperature increased with the diameter of the wood cylinder and the sand temperature. The observation of this temperature difference is a result of the difficulties in
235 releasing the exothermic heat through the poor heat conducting char. The overall heat transfer resistance increased with increasing distance (within the same particles in Figures 3 to 5 and among the particles of different diameters in Figure 6) from the outer surface, resulting the effective use of the heat from the exothermic reactions in increasing the local

temperature.

A major difference between the dry and the wet sample is the drying period where the temperature profile became flat until all the moisture was evaporated. During moisture evaporation at around 105°C inside the particle, the outer layers have reached higher temperatures where pyrolysis has started already. Many different types of reactions would have taken place at different locations within the same particle. As the steam from the centre or inner layers pass through the pyrolysing outer layers, it should affect the overall pyrolysis reaction as well as the product distribution. Tar and char yields along with some analysis results will be presented later to distinguish the difference between dry and wet sample pyrolysis.

3.2. Heating rate profiles within a pyrolysing particle: effects of moisture

In order to better identify the major thermal events during the pyrolysis of a large particle, the time-temperature profiles such as those shown in Figures 3 to 5 should be differentiated to show the heating rate profiles across the pyrolysing particle. Figures 7 to 10 show the typical heating rate profiles for the case of pre-set sand temperature of 400°C while those for the cases of pre-set sand temperatures of 300 and 350°C, showing qualitatively similar trends, are not shown here.

The reading from the thermocouple located radially 3 mm from the outer surface (Figure 7) would resemble the observation for a smaller particle. Figure 7 shows the presence of a major peak in heating rate centred around 100°C for both dry and moisture samples. Because the dry sample (Figure 7~~A~~, ~1 wt% moisture) has given a peak heating rate (~5.9~~7~~ K/s) that is much higher than that (2.2 K/s) of the moisture sample (in Figure 7~~B~~, 19.5 wt% moisture), the

main reason for this peak cannot be due to the water that might improve heat conductivity with increasing temperature. In fact, the presence of moisture in biomass has always reduced the height of this peak heating rate due to the endothermic heat required to evaporate the water.

Little weight loss is expected from the organic matter in biomass at temperatures lower than 100°C. Indeed, the "dry" sample was already dried at 105°C for 24 hours before the experiment. No non-negligible weight loss could possibly take place when the sample was re-heated to 100°C during the experiment. Therefore, no chemical reactions could possibly release such high amounts of energy to result in this large peak in heating rate at ~ 100°C. It is believed that the increases in the heating rate before 100°C were due to the increases in the thermal conductivity of biomass [21, 22], which speeded up the heat transfer process for increased heating rate as measured by the thermocouple. With increases in temperature at the location of thermocouple, the temperature difference driving the heat transfer from the sand bed to the location would have decreased, resulting in the slowdown of heating (i.e. reduced heating rate at 100°C). While the presence of moisture would tend to increase the heat conductivity and thus the heating rate, the heat demand to evaporate the moisture outweighed the effects of increased heat conductivity, to result in net decreases in heating rates for the wet sample compared with the dry sample.

Further moving into the biomass for the thermocouples located radially 6, 9 or ~12.5 (i.e. central) mm from the outer surface, the magnitude of this heating rate peak decreased (Figures 8 to 10). This is certainly because of the decreases in the temperature difference for heat transfer, increases in the distance of heat transfer and possibly the decreases in heat conductivity. At the time when the centre reached 100°C, the location at 3 mm from the outer surface had already reached >250°C. In other words, significant devolatilisation had taken

place with the biomass to result in a porous layer of char, which has low overall thermal conductivity. All these combined to reduce the observed heating rates with increasing distance from the outer surface.

While the evaporation of moisture at 3 mm in the biomass did not slow the heating down to zero heating rate (Figure 7, wet sample~~B~~), increasingly longer time was required to complete the evaporation of moisture at locations deeper into the biomass (Figures 8~~B~~ to 10, for wet samples~~B~~). At the centre (Figure 10, wet sample~~B~~), it took more than 140 s for the moisture to be evaporated (210 to 350 s) showing zero heating rate and constant temperature at 105°C. Obviously, heat transfer was the rate-limiting step for the evaporation of moisture from inside the biomass.

At the locations near the outer surface (e.g. 3 mm from the outer surface in Figure 7), there were only minor heating rate peaks at temperatures above 100-200°C region except from the drop in heating rate due to water evaporation at 105°C. The general trend is the decreases in heating rate with increasing temperature, mainly due to the decreases in temperature differences as the heat transfer driving force. Moving deeper into the biomass, the magnitudes of these peaks increased significantly. At the centre of the dry sample (Figure 10~~A~~), at least two additional heating rate peaks were observed at around 325°C and 425°C with~~and~~ a possible trough ~~were observed centred~~ at around ~~325°C,~~ 370°C ~~and 425°C~~. It is believed that these peaks reflect the possible exothermic reactions during pyrolysis. In fact, cellulose, hemicellulose and lignin can undergo exothermic degradation [23 – 25] in addition to the general endothermic nature of pyrolysis as well as some peak endothermic cellulose degradation reported around 360 to 370^{o}C [24 – 26].

The presence of moisture in the wet biomass has certainly complicated the thermal events observed. As is shown in Figures 10~~B~~ and, to lesser extents, in Figures 7~~B~~ to 9~~B~~, an

additional peak at around 200°C was observed for the wet biomass, which did not exist for the dry biomass. While the exact reasons remain unknown, two possible explanations are given here. Firstly, this may only be due to the "delayed" heating up because of moisture evaporation. As is shown in Figure 5B, inside the biomass where heat transfer is slow, the evaporation of moisture would stop the temperature from raising above 105°C. At around 190 s in Figure 5B, the temperatures at the locations of 6 mm, 9 mm and 12.6 mm (central) from the surface were practically all the same at ~ 105°C. At the end of moisture evaporation at the centre (as evidenced by temperature increase), at about 380-400s, the temperature difference between the 9 mm location and the centre was >50°C. This large temperature difference, coupled with the decreased energy demand because of the absence of moisture, would cause a rapid temperature increase, partially explaining the appearance of the peak heating rate at ~200°C.

The second possible reason for the extra heating rate peak at ~ 200°C is related to some chemical reactions. It is believed that the presence of moisture might have changed the non-covalent bonding forces in biomass and thus the reaction pathways. Wood has an oxygen content of ~ 45wt% [1, 2] in various functional groups in cellulose, hemicellulose, lignin and other components. The moisture in the biomass, via H-bonding and other non-covalent forces, will play an important role in determining the 3-D configurations of the macromolecules in the biomass. For the "dried" biomass sample, the 3-D configurations could change when the sample is cooled down. When the biomass is reheated up during pyrolysis, water was no longer part of the 3-D macromolecular network and the 3-D configuration may not recover completely. In other words, the 3-D configuration for the "wet" biomass at the time when moisture is removed at ~ 105°C may not be the same as that for the pre-"dried" biomass even if at the same temperature (>100°C). It is well known that the pyrolysis outcome

of biomass is dependent on the 3-D configuration. For example, the product distribution from cellulose would change with the micro-crystallinity of the cellulose substrate [27].

Two peak heating rates were observed at around 325 and 425°C. These exothermic reactions are more likely to be due to the condensation (bond-forming) reactions as opposed to the endothermic bond-breaking reactions. It is believed that the 325°C peak may be related to the condensation reactions to form a tighter char structure after the main thermal decomposition reactions of cellulose and hemicellulose. The 425°C peak may be related to the condensation reaction following the main bond breaking reactions of lignin.

3.3. Changed and unchanged nature of reactions due to moisture

As it is clear from the above discussion, the presence of moisture delays the heating up of biomass. It is necessary to understand if the nature of reactions has been changed by moisture in the biomass. A good way to achieve this would be to plot the heating rate as a function of temperature. Figure 11 compares the heating rate profiles for the wet sample with those of the dry sample at a pre-set sand temperature of 400°C.

Two important observations can be made from the figure. Firstly, the heating rate profile changed significantly with the location in the biomass for both wet and dry biomass samples. It would be wrong to assign all these differences to the possible differences in the nature of chemical reactions. For example, as was discussed above, the first peak is clearly due to the changes in the heat conductivity of biomass with temperature. The decreases in the size of this peak with increasing distance into the biomass are mainly due to the corresponding increases in the overall heat transfer resistance. For the same reasoning, the heat generated from exothermic reactions inside the biomass would become increasing difficult to dissipate

with increasing distance from the outer surface. Therefore, the exothermic peaks at 325°C and 425°C was the highest at the centre of the biomass.

Secondly, the wet biomass show a few differences from the dry biomass. In addition to the dip in heating rate at 105°C associated with the evaporation of moisture, an extra peak at around 200°C was observed. This has been discussed above. The thermal events at above 250°C were at least qualitatively similar for the wet and dry biomasses. Some minor differences exist between the two in terms of the magnitude of the peaks, particularly at 325°C. Figure 12 confirms that the thermal events inside the biomass did not change qualitatively with the sand temperature (the heat source) from 300 to 400°C, which agrees well with the literature report [16].

3.4. Effects of moisture on pyrolysis yields

The effects of moisture content can be further observed from the pyrolysis tar and char yields, as is shown in Table 1. The wet samples gave tar yields similar to (or slightly lower than) the dry ones at 300 and 350°C but lower tar yields at 400°C. Tar components were produced over a wide range of temperatures, from <300 to > 400°C. As is shown in Figure 5B, when moisture was released from the centre of the biomass (mainly from ~ 100 s to 380 s), the rest of the biomass cylinder was at temperatures from 100 to 380°C at which tar components were formed. In other words, the moisture released from the biomass cylinder centre would have to travel through a thick layer of pyrolysing biomass/char. The moisture could be intimately involved in the pyrolysis reactions. Some of these reactions have apparently resulted in some heavy tar radicals being bonded back to char, reducing the tar yield and increasing the char yield (Table 1). Our observation does not agree with the speculation

reported in the literature where moisture was thought to prevent the char forming reactions and stabilise the tar [9]. A further confirmation to our observation could be the comparison of levoglucosan yields between dry and wet samples (refer to Table 2) where it can be seen that the wet samples are producing significantly less levoglucosan at temperature above 300^{o}C.

While levoglucosan is prone to undergo further degradation in the presence of moisture at high temperature range (> 300°C), a little or no effect was found for some other (light) organics (refer to Table 2) in the tar.

3.5. UV-fluorescence of tar

UV-fluorescence spectra of tar samples produced at different reaction temperatures for dry and wet samples are presented in Figure 13. The same tar concentration of 4 ppm was used in recording the spectra shown in this figure. To facilitate comparison, the UV-fluorescence intensity was multiplied by the corresponding tar yield [28, 29] to express the fluorescence intensity on the basis of "per g of biomass", which in turn reflects the "relative yields" of aromatic ring systems. As was expected, increasing pyrolysis temperature has resulted in the formation and release of additional aromatic ring systems during the pyrolysis of dry samples.

Figures 13 show that the differences between the dry and wet samples were relatively lower at 300 and 350°C, but bigger at 400°C. Our previous work [3] showed that the UV-fluorescence intensity was directly related to the lignin-derived species. Therefore, the data in Figure 13 indicate that the moisture mainly affected the pyrolysis of lignin and less on cellulose/hemicellulose because the pyrolysis of the former takes place at high temperatures

than the latter [2].

4. Conclusions

From our study of temperature profiles during the pyrolysis of large mallee wood cylinders, it is confirmed that the initial peak in the heating-rate profiles around 100°C may be related to the increased thermal conductivity of wood. The presence of exothermic activities during the pyrolysis of large biomass particles is further confirmed in agreement with the literature. It is postulated that the exothermal peak around 325°C and 425°C may be related to the condensation (bond-forming) reactions following the degradation of biomass constituents.

By comparing the pyrolysis of dry and wet samples, it was confirmed that the moisture can potentially affect the overall pyrolysis reaction and product distribution. A new peak in the heating up profile around 200°C was observed during the pyrolysis of wet (high moisture content, 15 – 20 wt%) samples. One of the possible reasons may be the increased temperature gradient, which triggered the jump in the heating rate profile once moisture evaporation was finished in the inner layers of the biomass particle. Another possible reason may be the difference in 3-D configuration of the macromolecules of biomass due to in-situ moisture evaporation compared to the pre-“dried” biomass sample. Moisture in the pyrolysing biomass has been found affecting the product distribution by encouraging char formation from heavy tar radicals.

Acknowledgments

This project has received funding from ARENA as part of ARENA's Emerging Renewables Program and the Second Generation Biofuels Research and Development Grant Program. The study also received support from the Government of Western Australia via the Low Emissions Energy Development Fund and via the Centre for Research into Energy for Sustainable Transport (CREST). This project is also supported by the Commonwealth of Australia under the Australia-China Science and Research Fund. This research used large samples of mallee biomass supplied without cost by David Pass and Wendy Hobley from their property in the West Brookton district.

References

1. J. Shen, X-S. Wang, M. Garcia-Perez, D. Mourant, M. J. Rhodes, C-Z. Li. Effect of particle size on the fast pyrolysis of oil mallee woody biomass. Fuel 88 (2009) 1810 – 1817.
2. M. Garcia-Perez, X-S. Wang, J. Shen, M. J. Rhodes, F. Tian, W-J. Lee, H. Wu, C-Z. Li. Fast pyrolysis of oil mallee woody biomass: Effect of temperature on the yield and quality of pyrolysis products. Ind. Eng. Chem. Res. 47 (2008) 1846 – 1854.
3. M. Garcia-Perez, S. Wang, J. Shen, M. Rhodes, W. J. Lee, C-Z. Li. Effects of temperature on the formation of lignin-derived oligomers during the fast pyrolysis of mallee woody biomass. Energy & Fuels 22 (2008) 2022 – 2032.
4. O. Beaumont, Y. Schwob. Influence of physical and chemical parameters on wood pyrolysis. Ind. Eng. Chem. Process Des. Dev. 23 (1984) 637 – 641.
5. A. V. Bridgwater, D. Meier, D. Radlein. An overview of fast pyrolysis of biomass. Organic Geochemistry 30 (1999) 1479 – 1493.

6. C. Di Blasi, C. Branca. Temperatures of wood particles in a hot sand bed fluidized by nitrogen. Energy & Fuels 17 (2003) 247 – 254.
7. X. Wang, S. R. A. Kersten, W. Prins, W. P. M. van Swaaij. Biomass pyrolysis in a fluidized bed Reactor. Part 2: Experimental validation of model results. Ind. Eng. Chem. Res. 44 (2005) 8786 – 8795.
8. C. Di Blasi, C. Branca, A. Santoro, E. G. Hernandez. Pyrolytic behaviour and products of some wood varieties. Combustion and Flame 124 (2001) 165 – 177.
9. W. C. R. Chan, M. Kelbon, B. Krieger-Brockett. Single-particle biomass pyrolysis: correlations of reaction products with process conditions. Ind. Eng. Chem. Res. 27 (1988) 2261 – 2275.
10. R. Bilbao, A. Millera, M. B. Murillo. Temperature profiles and weight loss in the thermal decomposition of large spherical wood particles. Ind. Eng. Chem. Res. 32 (1993) 1811 – 1817.
11. W. C. Park, A. Atreya, H. R. Baum. Experimental and theoretical investigation of heat and mass transfer processes during wood pyrolysis. Combustion and Flame 157 (2010) 481-494.
12. H. Bennadji, K. Smith, S. Shabangu, E. M. Fisher. Low-temperature pyrolysis of woody biomass in the thermally thick regime. Energy & Fuels 27 (2013) 1453-1459.
13. M. J. J. Antal, G. Varhegyi. Cellulose Pyrolysis Kinetics: The current state of knowledge. Ind. Eng. Chem. Res. 34 (1995) 703-717.
14. C. Di Blasi. Modelling intra- and extra- particle processes of wood fast pyrolysis. AIChE J. 48 (2002) 2386-2397.
15. Y. Haseli, J. A. van Oijen, L. P. H. de Goey. Modeling biomass particle pyrolysis with temperature-dependent heat of reactions. Journal of Analytical and Applied Pyrolysis 90 (2011) 140-154.
16. C. Di Blasi, C. Branca, F. Masotta, E, De Biase. Experimental analysis of reaction heat effects during beech wood pyrolysis. Energy & Fuels 27 (2013) 2665-2674.
17. D. Mourant, Z. Wang, M. He, X. S. Wang, M. Garcia-Perez, K. Ling, C-Z. Li. Mallee wood fast pyrolysis: effects of alkali and alkaline earth metallic species on the yield and composition of bio-oil. Fuel 90 (2011) 2915-2922.
18. Z. Min, M. Asadullah, P. Yimsiri, S. Zhang, H. Wu, C-Z. Li. Catalytic reforming of tar during gasification. Part I. Steam reforming of biomass tar using ilmenite as a catalyst.

Fuel 90 (2011) 1847-1854.

19. R. Gunawan, X. Li, A. Larcher, X. Hu, D. Mourant, W. Chaiwat, H. Wu, C-Z. Li. Hydrolysis and glycosidation of sugars during the esterification of fast pyrolysis bio-oil. Fuel 95 (2012) 146-151.
20. X. Hu, R. Gunawan, D. Mourant, C. Lievens, X. Li, S. Zhang, W. Chaiwat, C-Z. Li. Acid-catalysed reactions between methanol and bio-oil from the fast pyrolysis of mallee bark. Fuel 97 (2012) 512-522.
21. H. P. Steinhagen. Thermal conductive properties of wood, green or dry, from -40° to +100° C: A literature review. USDA FOREST SERVICE, GENERAL TECHNICAL REPORT, FPL 9, 1977.
22. Z-T. Yu, X. Xu, L-W. Fan, Y-C. Hu, K-F. Cen. Experimental measurements of thermal conductivity of wood species in China: effect of density, temperature, and moisture content. FOREST PRODUCTS JOURNAL 61 (2011) 130-135.
23. M. V. Ramiah. Thermogravimetric and differential thermal analysis of cellulose, hemicellulose and lignin. Journal of Applied Polymer Science 14 (1970) 1323-1337.
24. H. Yang, R. Yan, H. Chen, C. Zheng, D. H. Lee, D. T. Liang. In-depth investigation of biomass pyrolysis based on three major components: hemicelluloses, cellulose and lignin. Energy & Fuels 20 (2006) 388 – 393.
25. D. F. Arseneau. Competitive reactions in thermal decomposition of cellulose. Canadian Journal of Chemistry 49 (1971) 632-638.
26. D. K. Shen, S. Gu, A. V. Bridgwater. The thermal performance of the polysaccharides extracted from hardwood: Cellulose and hemicelluloses. Carbohydrate Polymers 8 (2010) 39 – 45.
27. Z. Wang, A. G. McDonald, R. J. M. Westerhof, S. R. A. Kersten, C. M. Cuba-Torres, S. Ha, B. Pecha, M. Garcia-Perez. Effect of cellulose crystallinity on the formation of a liquid intermediate and on product distribution during pyrolysis. Journal of Analytical and Applied Pyrolysis 100 (2013) 56-66.
28. C-Z Li, C. Sathe, J. R. Kershaw, Y. Pang. Fates and roles of alkali and alkaline earth metals during the pyrolysis of a Victorian brown coal. Fuel 79 (2000) 427-438.
29. J. R. Kershaw, C. Sathe, J-I. Hayashi, C-Z. Li, T. Chiba. Fluorescence spectroscopic analysis of tars from the pyrolysis of a Victorian brown coal in a wire-mesh reactor. Energy & Fuels 14 (2000) 476-482.

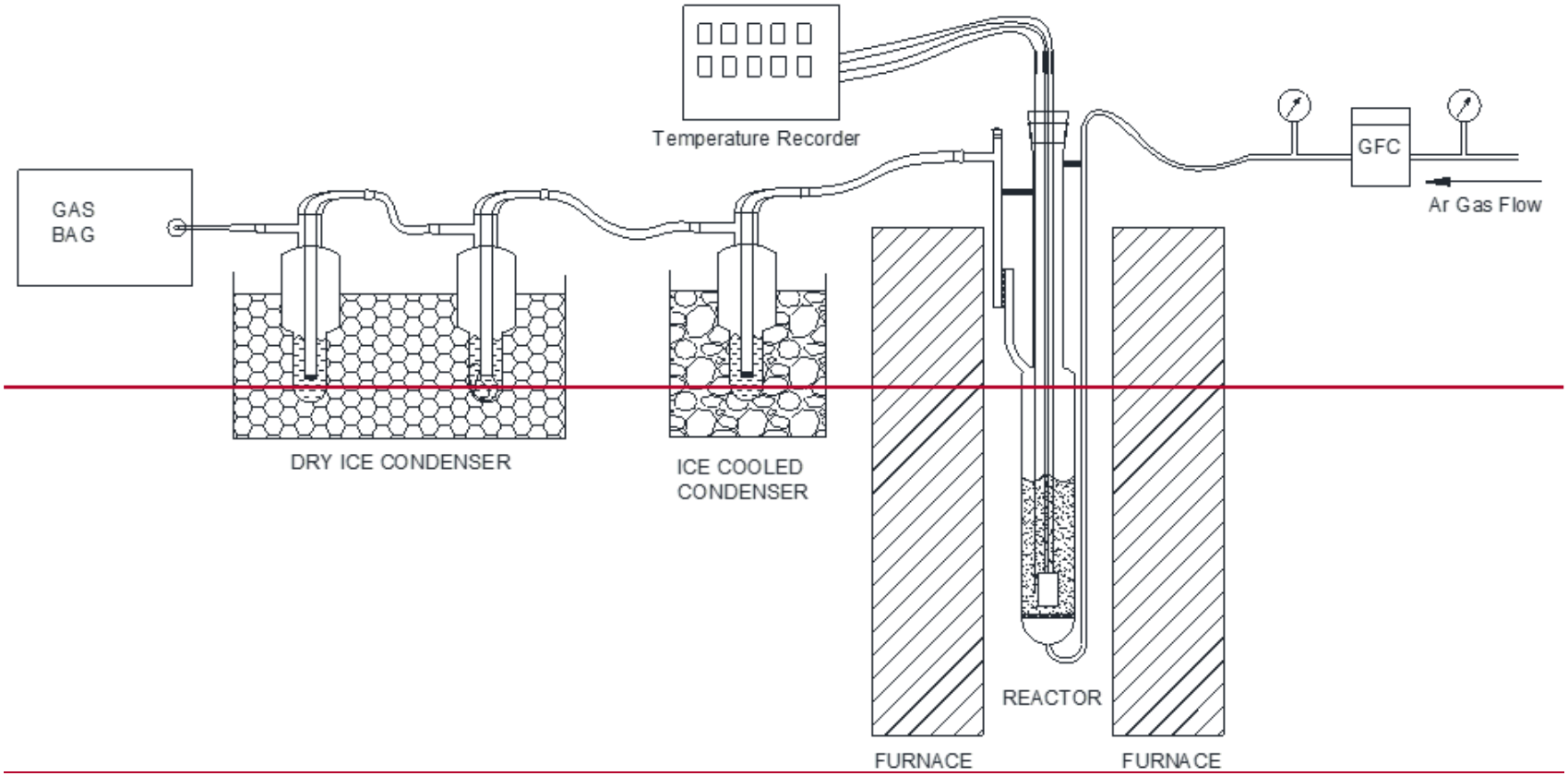
Temperature Recorder
GAS
BAG
GFC
Ar Gas Flow
DRY ICE CONDENSER
ICE COOLED
CONDENSER
REACTOR
FURNACE
FURNACE

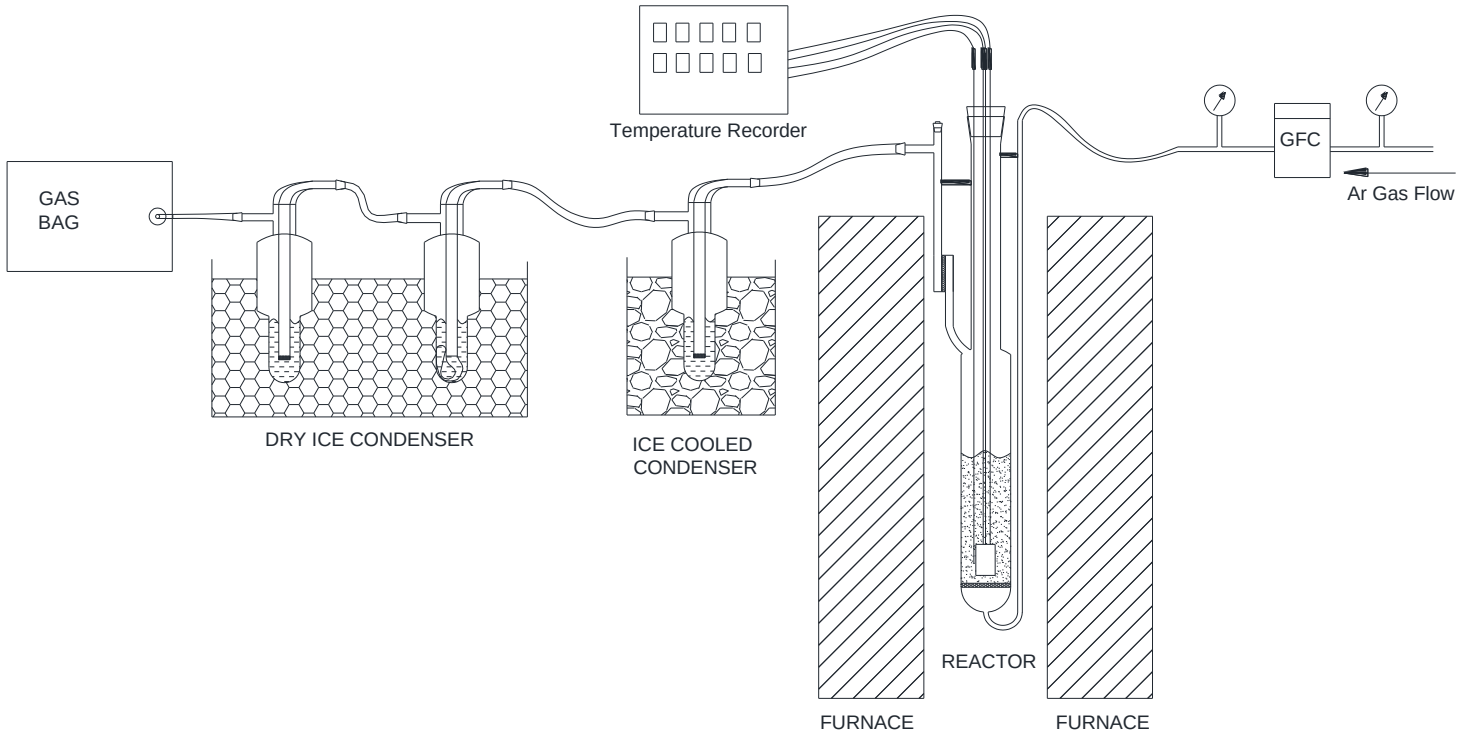

Figure 1. A schematic diagram of the experimental setup for the pyrolysis of single wood particles.

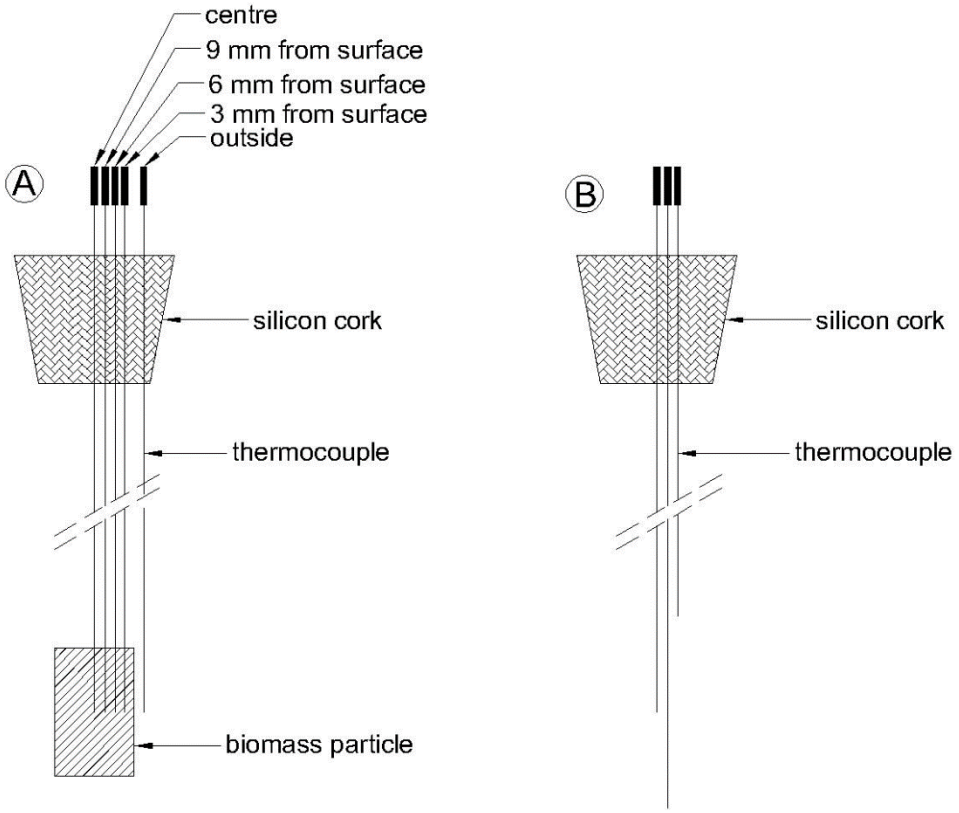

Figure 2. Thermocouple assemblies used during a pyrolysis experiment. (A), a set of thermocouples used to measure the temperature at different radial positions inside a pyrolysing sample; (B), a set of thermocouples used to monitor the temperature of the fluidised bed during heating up.

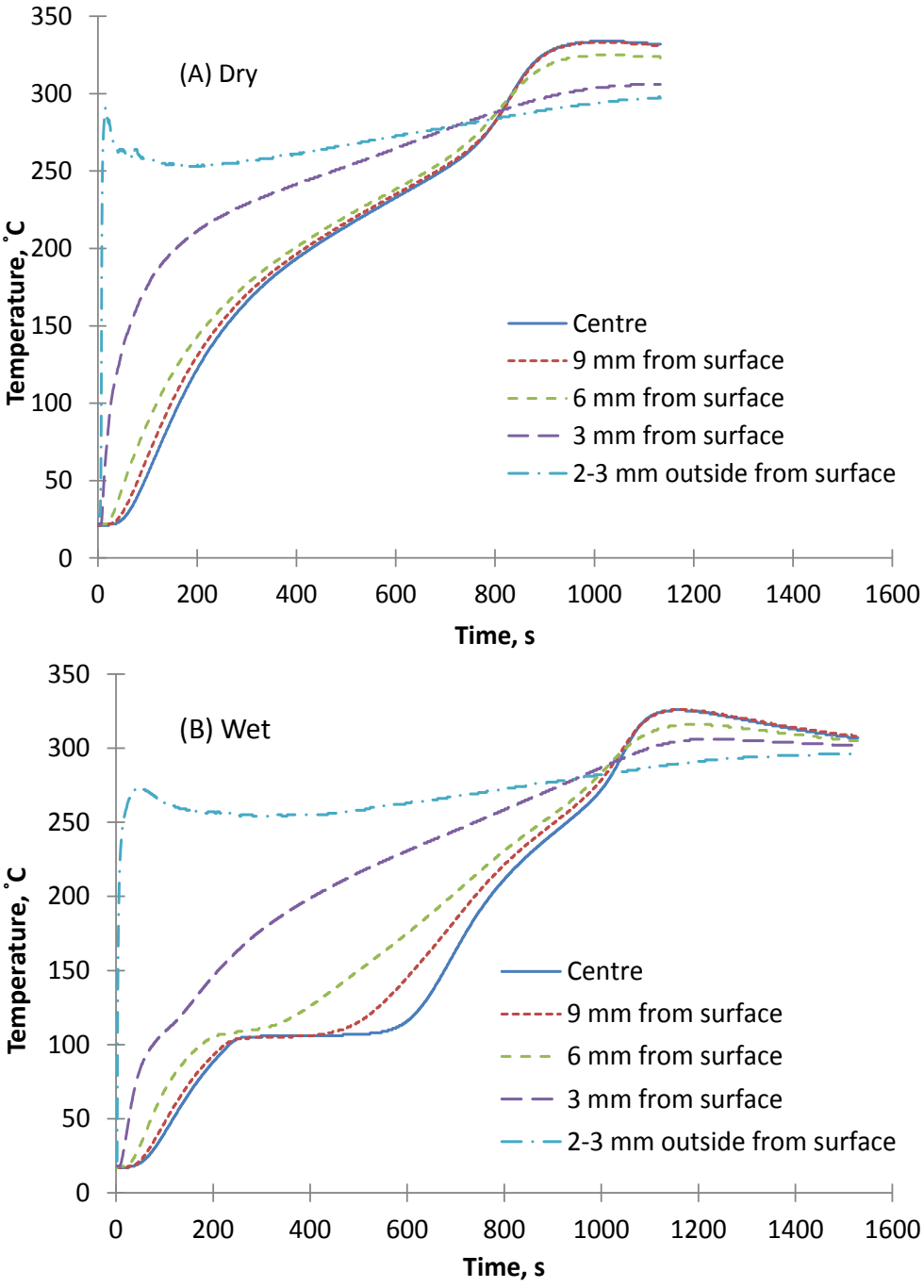

Figure 3. Temperature profiles in a pyrolysing wood cylinder at a pre-set sand bed temperature of 300°C. (A), a dry cylinder with a diameter of 25.1 mm; (B), a wet wood cylinder with a diameter of 25.4 mm and a 20.1% moisture content.

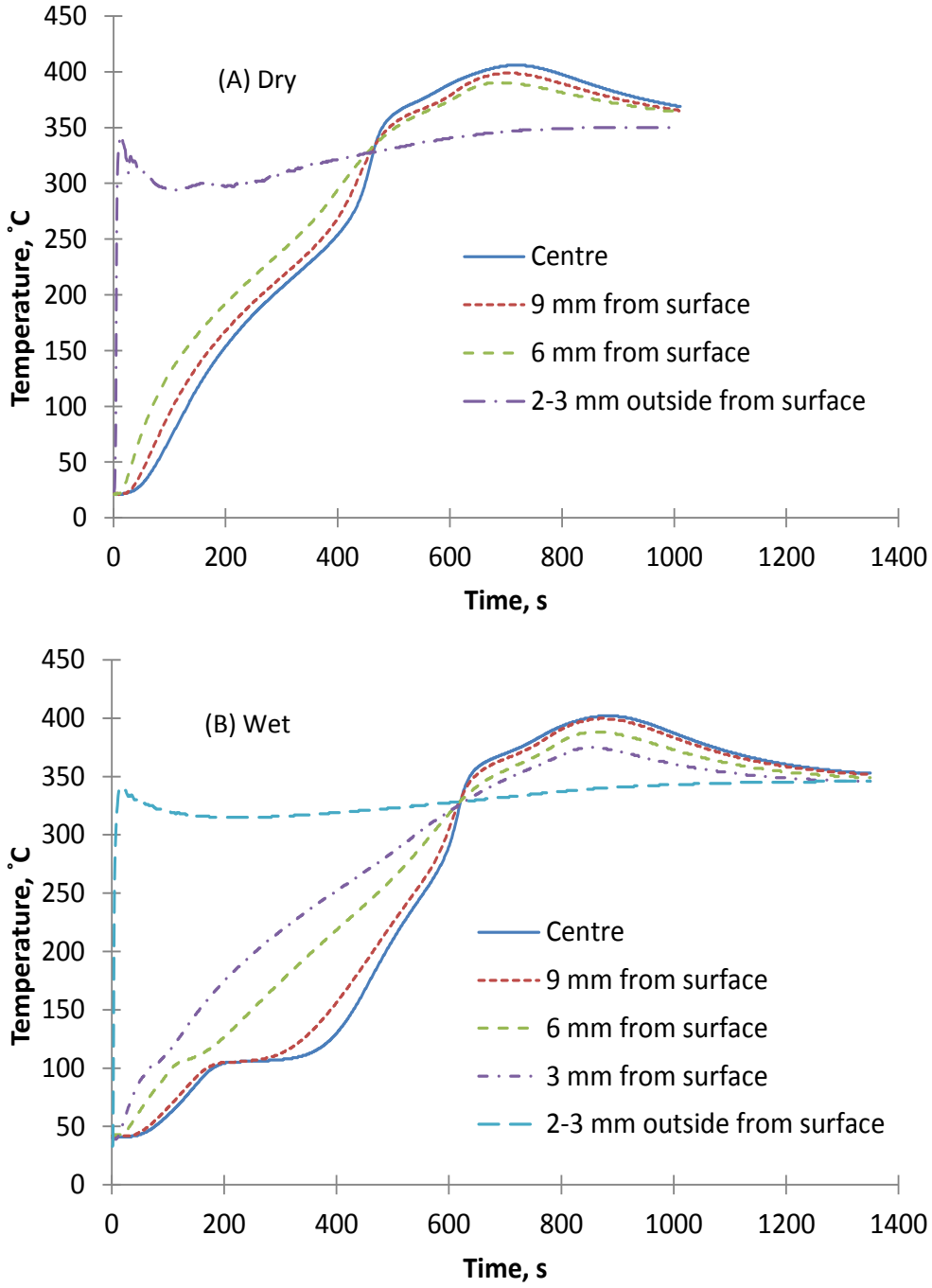

Figure 4. Temperature profiles in a pyrolysing wood cylinder at a pre-set sand bed temperature of 350°C. (A), a dry cylinder with a diameter of 25.4 mm; (B), a wet wood cylinder with a diameter of 25.4 mm and a 15.9% moisture content.

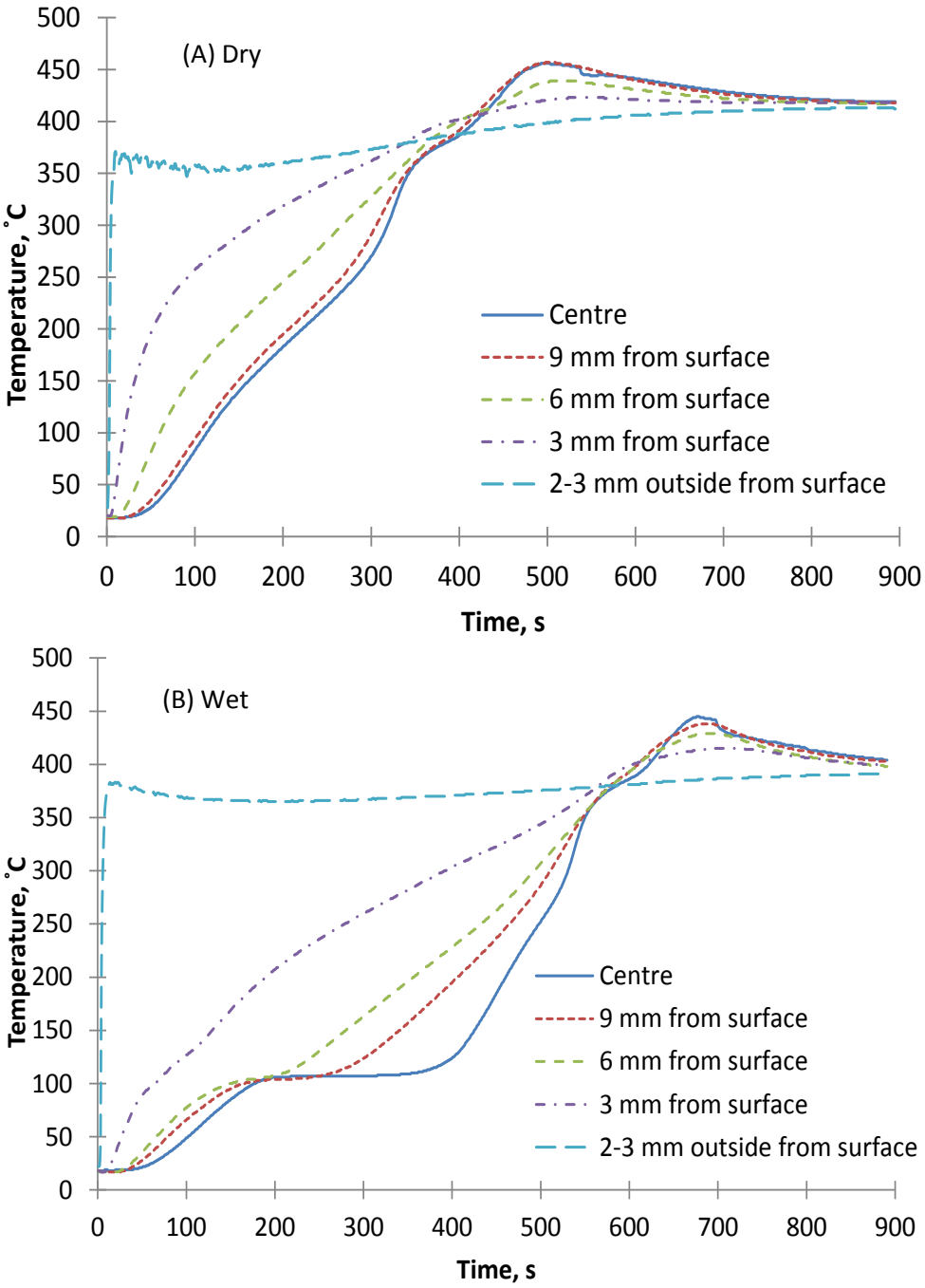

Figure 5. Temperature profiles in a pyrolysing wood cylinder at a pre-set sand bed temperature of 400°C. (A), a dry cylinder with a diameter of 24.4 mm; (B), a wet wood cylinder with a diameter of 25.1 mm and a 19.5% moisture content.

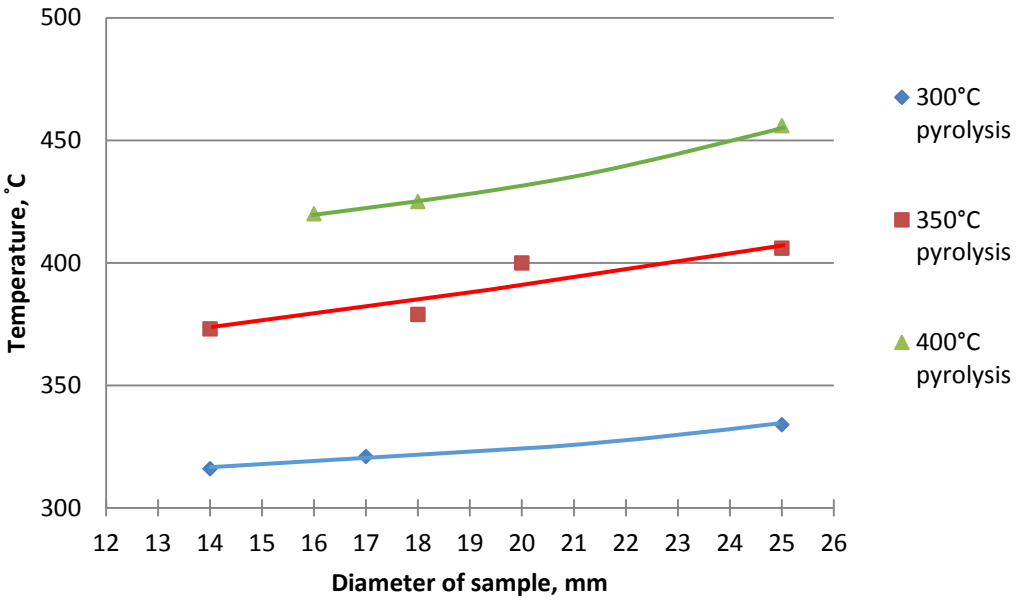

Figure 6. Peak temperature at the centre of the pyrolysing biomass as a function of sample diameter at different reaction (sand) temperatures.

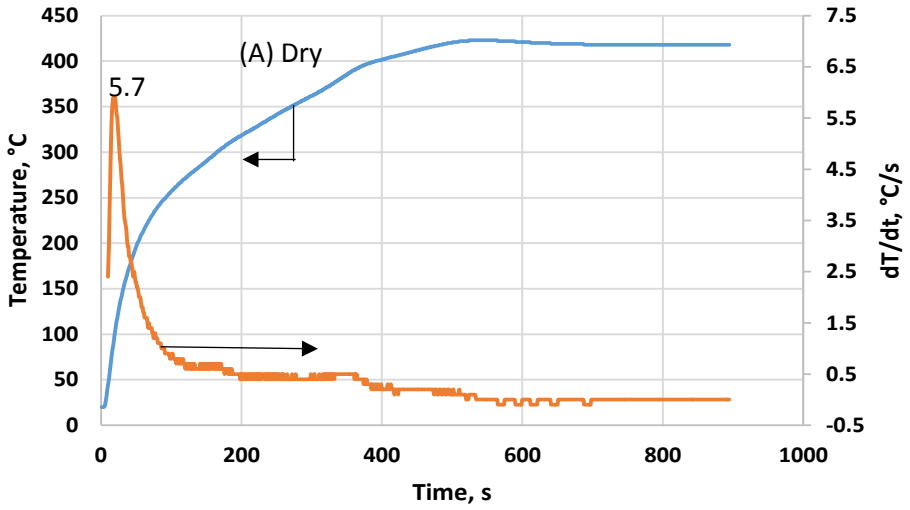
(A) Dry
5.7
Temperature, °C
dT/dt, °C/s
Time, s
0
50
100
150
200
250
300
350
400
450
-0.5
0.5
1.5
2.5
3.5
4.5
5.5
6.5
7.5
0
200
400
600
800
1000

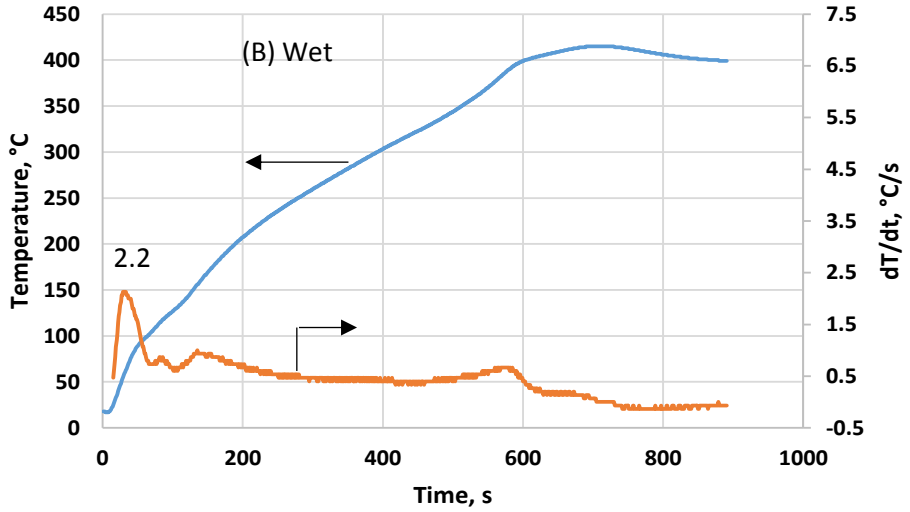
(B) Wet
2.2
Temperature, °C
dT/dt, °C/s
Time, s
0
50
100
150
200
250
300
350
400
450
-0.5
0.5
1.5
2.5
3.5
4.5
5.5
6.5
7.5
0
200
400
600
800
1000

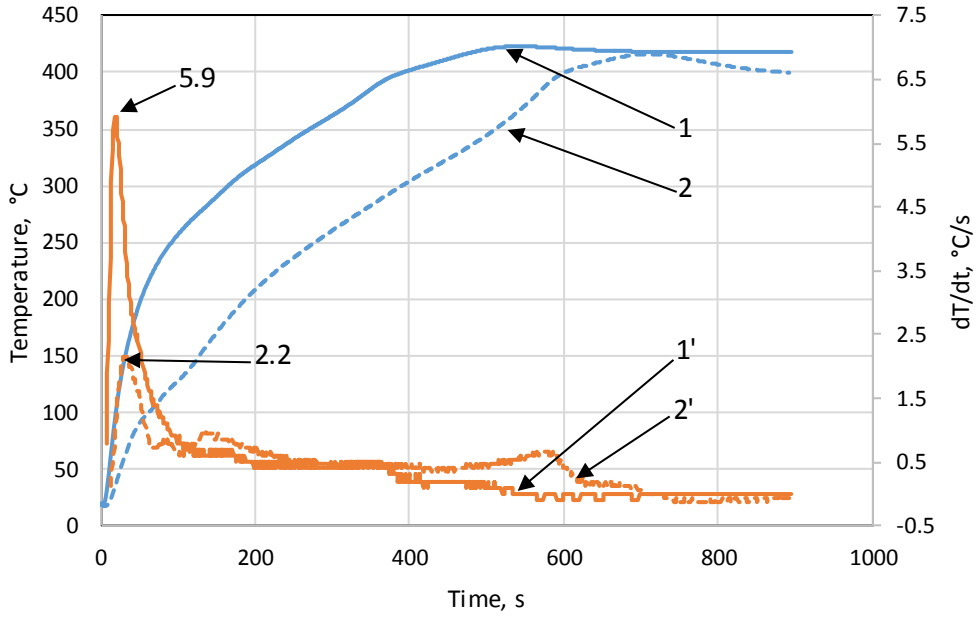
5.9
1
2
2.2
1'
2'
Temperature, °C
dT/dt, °C/s
Time, s
0
50
100
150
200
250
300
350
400
450
-0.5
0.5
1.5
2.5
3.5
4.5
5.5
6.5
7.5
0
200
400
600
800
1000

Figure 7. Temperature profile at 3 mm and its time derivatives plotted against time for samples pyrolysed at 400°C. (~~A~~1), temperature profile for dry sample; (~~B~~2), temperature profile for wet sample; (1'), derivative temperature profile for dry sample; (2'), derivative temperature profile for wet sample.

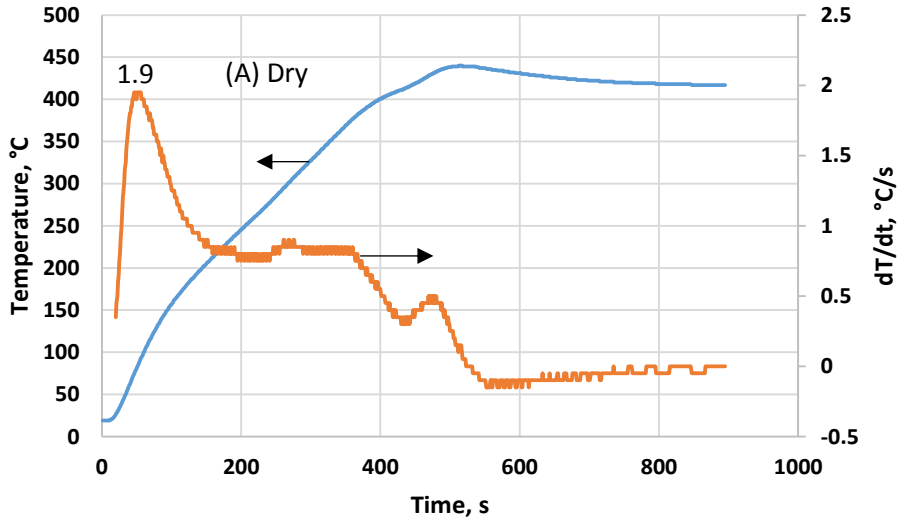
1.9
(A) Dry
Temperature, °C
dT/dt, °C/s
Time, s
0
50
100
150
200
250
300
350
400
450
500
-0.5
0
0.5
1
1.5
2
2.5
0
200
400
600
800
1000

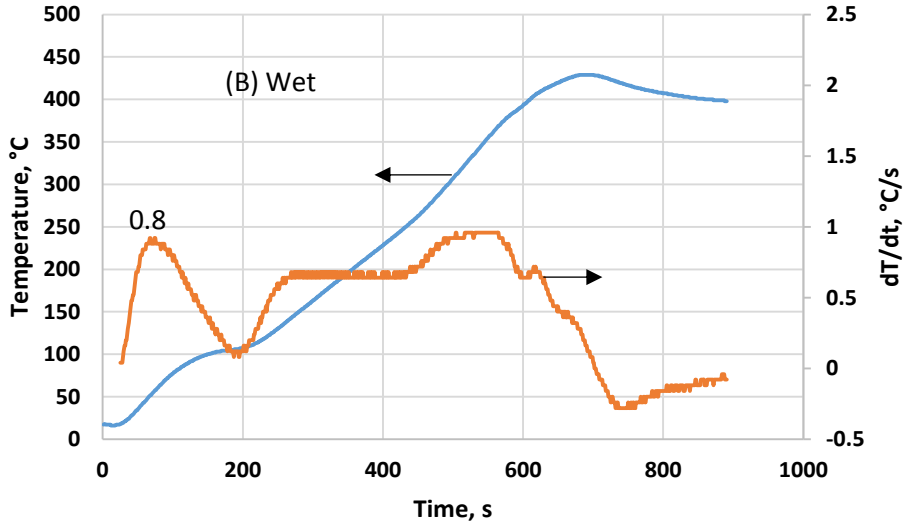
(B) Wet
0.8
Temperature, °C
dT/dt, °C/s
Time, s
0
50
100
150
200
250
300
350
400
450
500
-0.5
0
0.5
1
1.5
2
2.5
0
200
400
600
800
1000

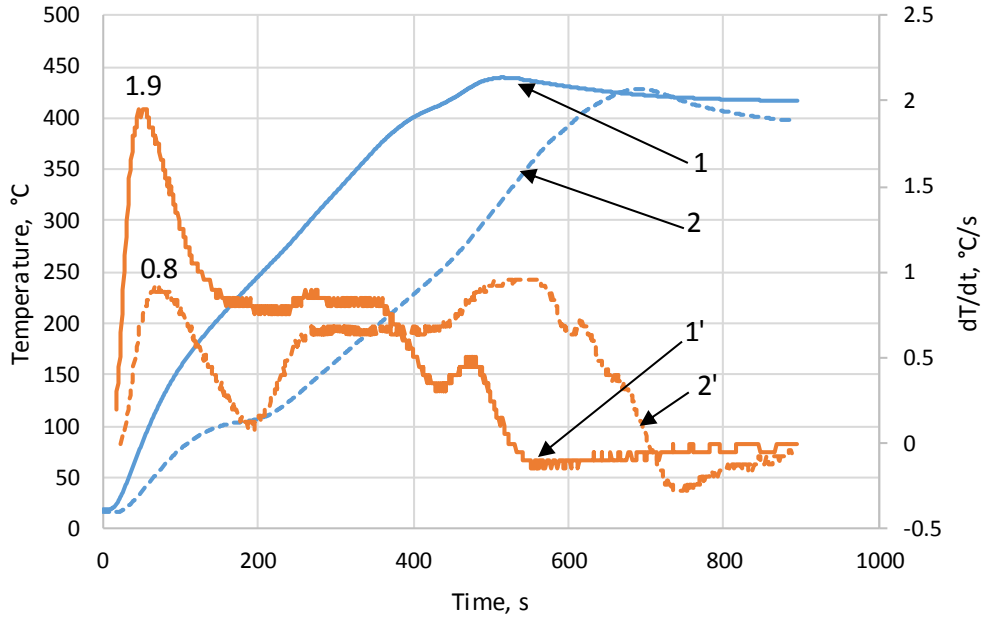
1.9
0.8
1
2
1'
2'
Temperature, °C
dT/dt, °C/s
Time, s
0
50
100
150
200
250
300
350
400
450
500
-0.5
0
0.5
1
1.5
2
2.5
0
200
400
600
800
1000

Figure 8. Temperature profile at 6 mm and its time derivatives plotted against time for samples pyrolysed at 400°C. (1), temperature profile for dry sample; (2), temperature profile for wet sample; (1'), derivative temperature profile for dry sample; (2'), derivative temperature profile for wet sample~~(A), dry sample; (B), wet sample~~.

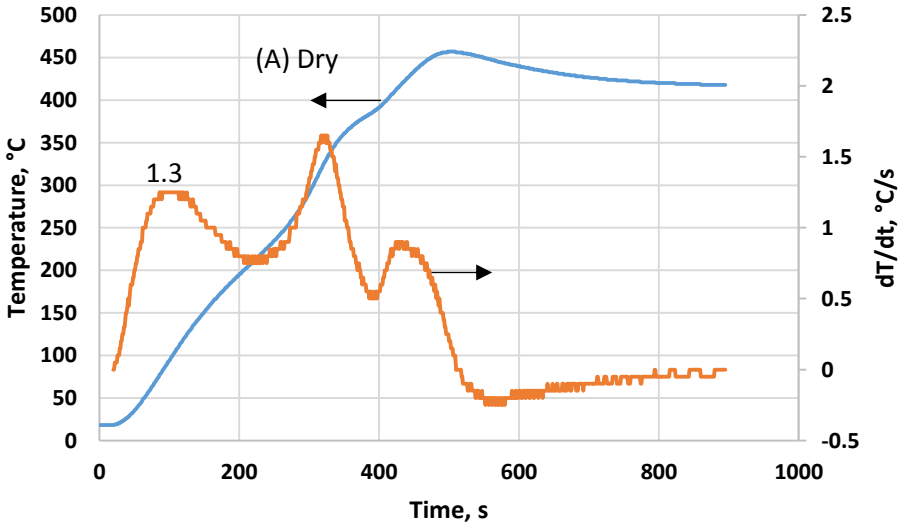
(A) Dry
1.3
Temperature, °C
dT/dt, °C/s
Time, s
0
50
100
150
200
250
300
350
400
450
500
-0.5
0
0.5
1
1.5
2
2.5
0
200
400
600
800
1000

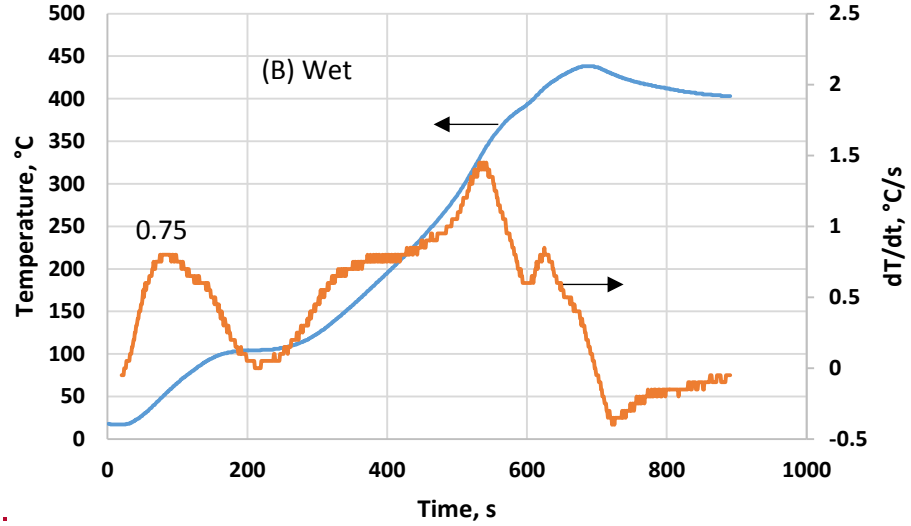
(B) Wet
0.75
Temperature, °C
dT/dt, °C/s
Time, s
0
50
100
150
200
250
300
350
400
450
500
-0.5
0
0.5
1
1.5
2
2.5
0
200
400
600
800
1000

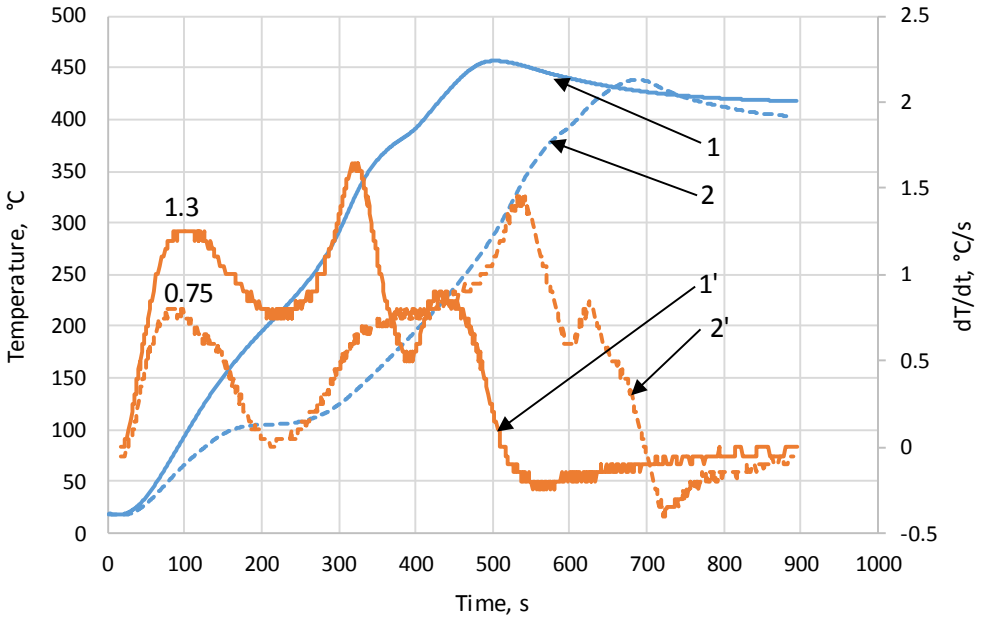
1.3
0.75
1
2
1'
2'
Temperature, °C
dT/dt, °C/s
Time, s
0
50
100
150
200
250
300
350
400
450
500
-0.5
0
0.5
1
1.5
2
2.5
0
100
200
300
400
500
600
700
800
900
1000

Figure 9. Temperature profile at 9 mm and its time derivatives plotted against time for samples pyrolysed at 400°C. (1), temperature profile for dry sample; (2), temperature profile for wet sample; (1'), derivative temperature profile for dry sample; (2'), derivative temperature profile for wet sample~~(A), dry sample; (B), wet sample~~.

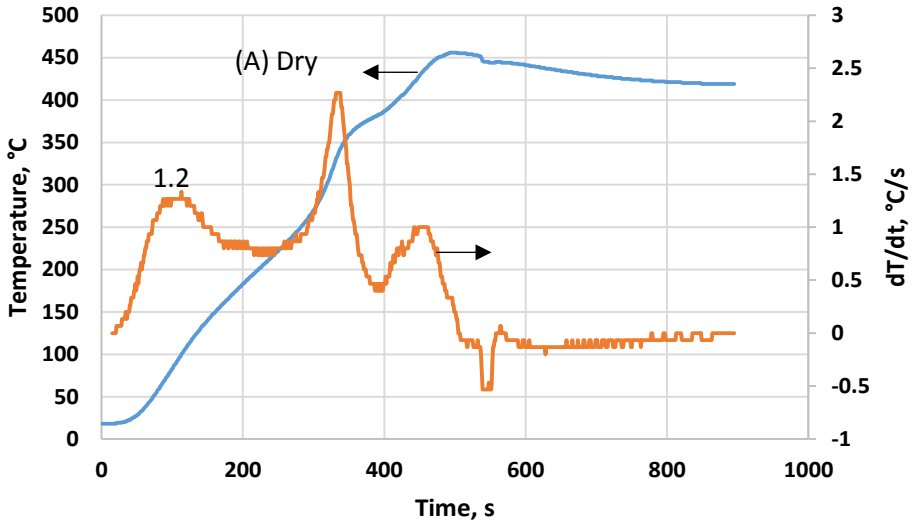
(A) Dry
1.2
Temperature, °C
dT/dt, °C/s
Time, s
0
50
100
150
200
250
300
350
400
450
500
-1
-0.5
0
0.5
1
1.5
2
2.5
3
0
200
400
600
800
1000

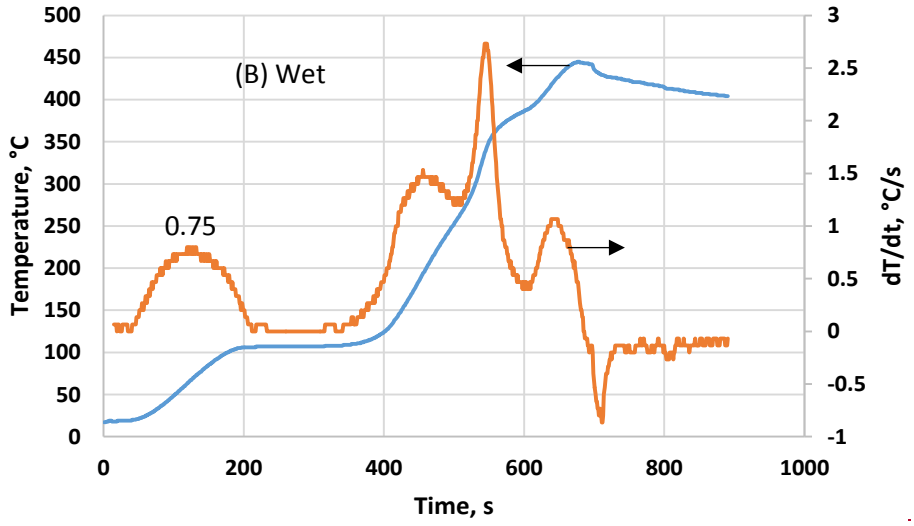
(B) Wet
0.75
Temperature, °C
dT/dt, °C/s
Time, s
0
50
100
150
200
250
300
350
400
450
500
-1
-0.5
0
0.5
1
1.5
2
2.5
3
0
200
400
600
800
1000

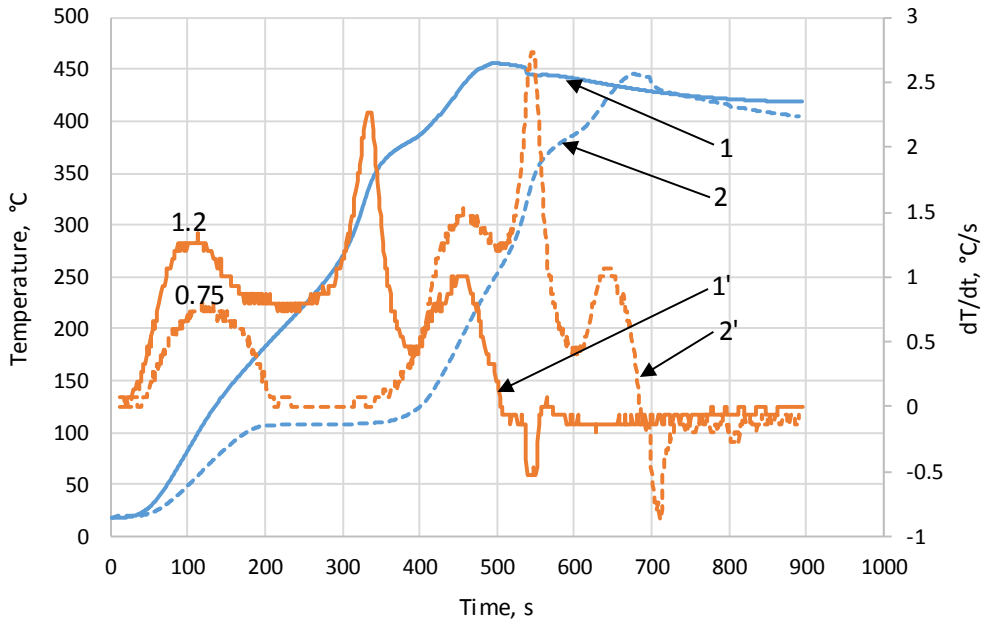
1
2
1'
2'
1.2
0.75
Temperature, °C
dT/dt, °C/s
Time, s
0
50
100
150
200
250
300
350
400
450
500
-1
-0.5
0
0.5
1
1.5
2
2.5
3
0
100
200
300
400
500
600
700
800
900
1000

Figure 10. Temperature profile at the centre and its time derivatives plotted against time for samples pyrolysed at 400°C. (1), temperature profile for dry sample; (2), temperature profile for wet sample; (1'), derivative temperature profile for dry sample; (2'), derivative temperature profile for wet sample~~(A), dry sample; (B), wet sample~~.

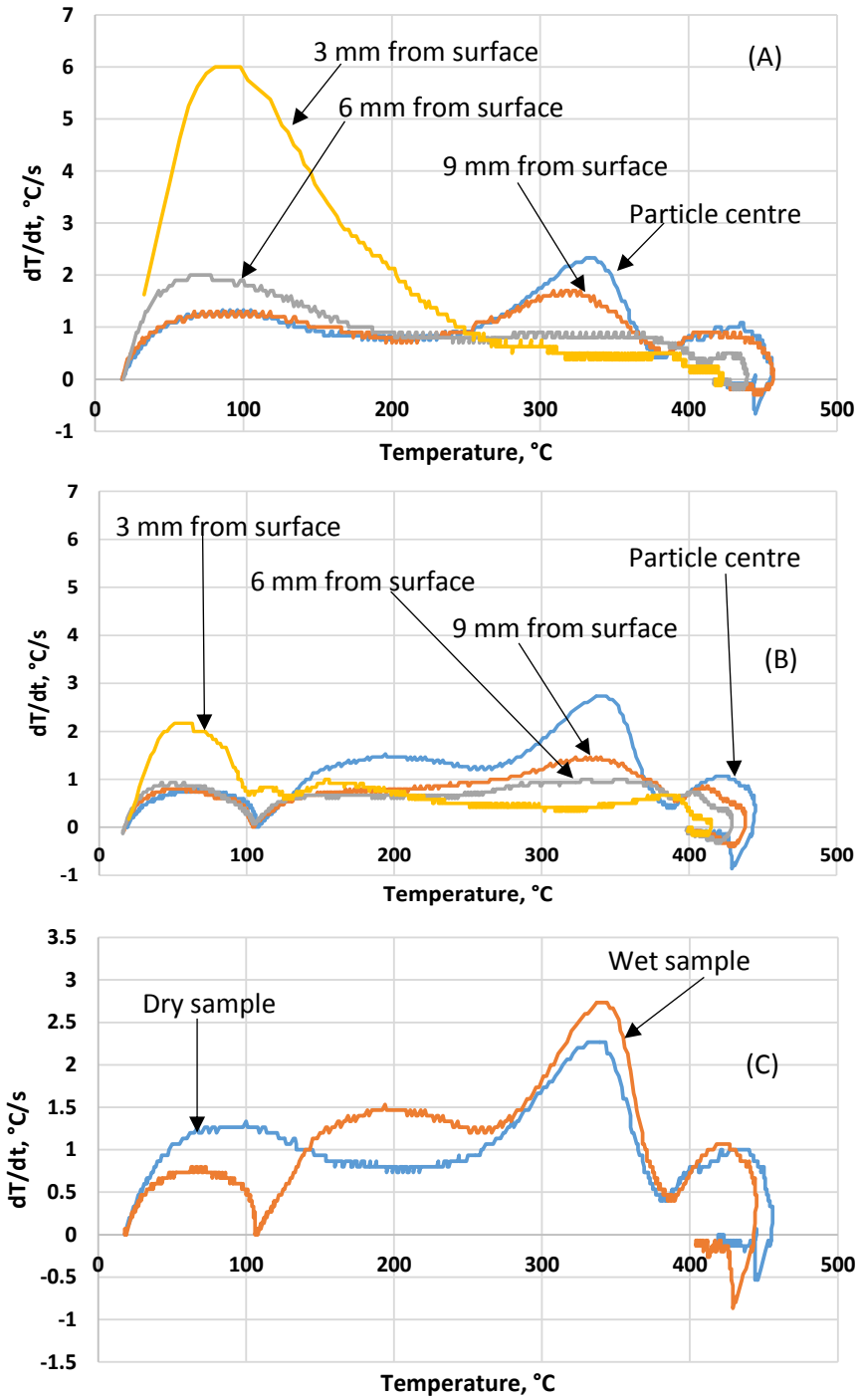

Figure 11. Heating rate profiles as a function of radial position into the biomass and temperature for the pyrolysis at a sand temperature of 400°C. (A), dry sample; (B), wet sample; (C), comparison between centre profiles.

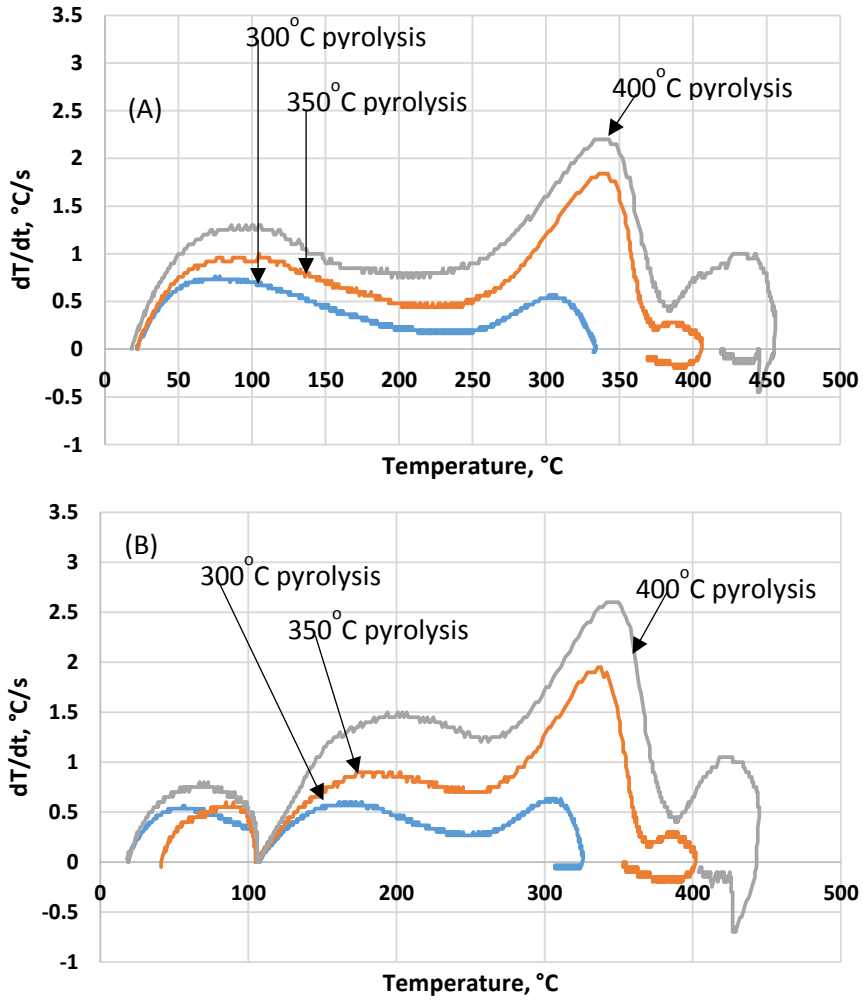

Figure 12. Heating rates at the centre of biomass as a function of temperature. (A), dry sample; (B), wet sample.

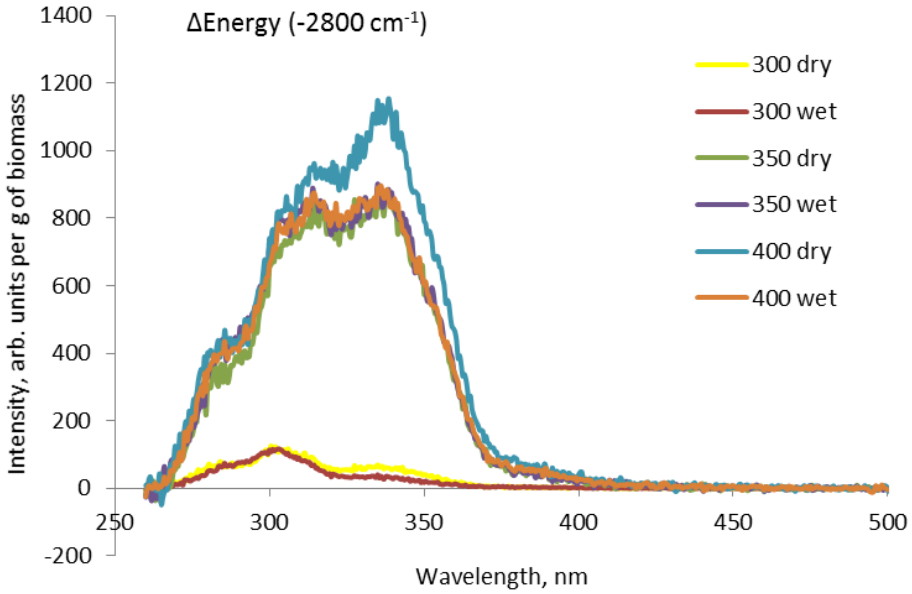

Figure 13. Comparison of UV fluorescence spectra of tar samples produced from the pyrolysis of dry and wet samples at different temperatures.

Table 1. Comparison of tar and char yields produced from dry and wet samples under different pyrolysis temperatures.

Pyrolysis temperature, °C	Tar yield, wt% dry biomass		Char yield, wt% dry biomass	
	Dry sample	Wet sample	Dry sample	Wet sample
400	20.52	16.04	31.18	35.19
400	21.41	-	31.64	-
350	18.35	16.28	36.28	39.49
350	16.49	16.1	37.86	38.39
300	4.66	3.58	69.23	75.34
300	5.3	4.5	69.87	80.18

Table 2. Comparison of yields (dry biomass basis) of various components of tar produced from dry and wet samples under different pyrolysis temperatures.

Pyrolysis temperature, °C	Yields of levoglucosan, wt%		Yields of furfural, wt%		Yields of furfuryl alcohol, wt%		Yields of methoxy eugenol, wt%		Yields of syringol, wt%	
	Dry	Wet	Dry	Wet	Dry	Wet	Dry	Wet	Dry	Wet
300	0.04	0.01	0.41	0.40	0.07	0.03	0.02	0.02	0.21	0.18
350	0.97	0.31	0.53	0.48	0.29	0.24	0.05	0.04	0.67	0.61
375	1.01	0.57	0.52	0.52	0.29	0.26	0.06	0.05	0.79	0.78
400	1.16	0.60	0.51	0.56	0.30	0.23	0.06	0.05	0.73	0.83